Cellulose (2019) 26:2233–2242
https://doi.org/10.1007/s10570-018-02238-3

ORIGINAL RESEARCH

Intrinsic characteristics of cellulose dissolved in an ionic liquid: the shape of a single cellulose molecule in solution

Mitsuharu Koide · Isao Wataoka · Hiroshi Urakawa · Kanji Kajiwara · Ute Henniges · Thomas Rosenau

Received: 9 October 2018 / Accepted: 29 December 2018 / Published online: 2 January 2019

Abstract Although cellulose is the oldest macromolecule we have known, its intrinsic properties are still not well understood because of the lack of suitable solvents. The recent development of ionic liquids enables preparation of cellulose solutions in which cellulose molecules are supposed to be dispersed molecularly. Conventionally a semi-flexible-chain model or a worm-like chain model has been applied to describe the dilute solution properties of cellulose. A semi-flexible chain model is specified in terms of a persistent length to determine the chain stiffness of a solute molecule, completely neglecting details of the solvent–solute interaction, and the discussion is mainly focusing on the conformation of a solute molecule. In this paper we adapt a cylinder model which at least specifies the local shape of a solute molecule. Since the ionic liquids are now available as a new solvent of cellulose, we have prepared cellulose/ionic liquid solutions for small-angle X-ray scattering (SAXS) measurements which provide information on the local structure of cellulose molecules in the restricted range. The SAXS measurements were performed on the cellulose/ionic liquid solutions at two independent synchrotron facilities and confirmed the consistency of the observed scattering profile. Standard methods were applied to analyze the scattered data first, and afforded a model for representing a cellulose molecule in ionic liquid solutions. Two types of ionic liquids were used, and it was ascertained that cellulose was not degraded under the conditions used. The solution characteristic was found to change by heating during the preparation of each solution. The heating effect on the conformational change of cellulose was discussed in terms of the solute–solvent interaction from the simulation with a coaxial double layer cylinder model. The state of solvent packing was considered as well from the thickness and relative electron density of the sheath in the simulated coaxial double layer cylinder model.

M. Koide · U. Henniges · T. Rosenau
Division of Chemistry of Renewables, Department of Chemistry, University of Natural Resources and Life Sciences, Vienna (BOKU), Muthgasse 18, 1190 Vienna, Austria

I. Wataoka (✉) · H. Urakawa
Department of Biobased Materials Science, Faculty of Fiber Science and Engineering, Kyoto Institute of Technology, Matsugasaki, Sakyo-ku, Kyoto City, Kyoto 6068585, Japan
e-mail: wataoka@kit.ac.jp

K. Kajiwara
Faculty of Textile Science and Technology, Shinshu University, 3-15-1 Tokida, Ueda City, Nagano 3868567, Japan

T. Rosenau
Johan Gadolin Process Chemistry Centre, Åbo Akademi University, Porthansgatan 3, 20500 Åbo, Turku, Finland

Graphical abstract

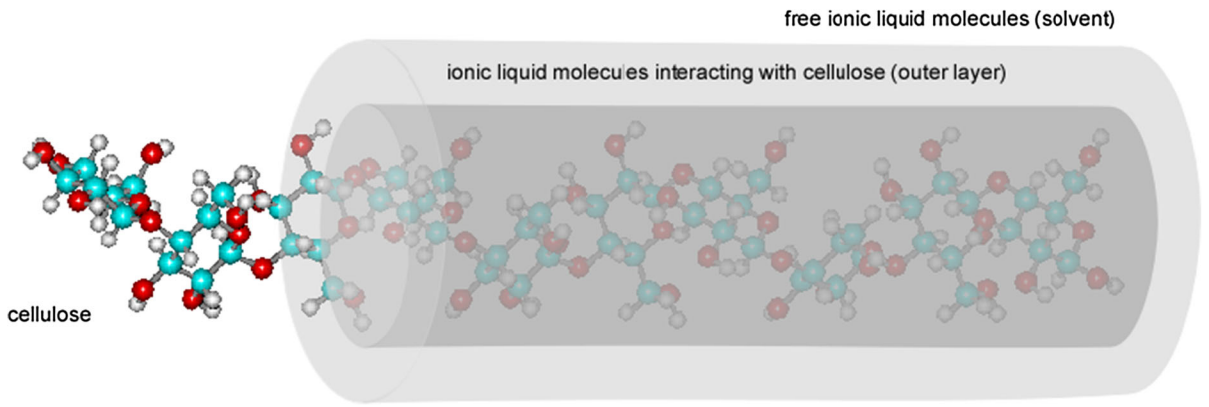

Keywords Cellulose · Cellulose degradation · Cellulose solution · Coaxial double cylinder model · Ionic liquids · Small-angle X-ray scattering

Introduction

Cellulose is one of the most abundantly available structural materials, which has come to play a key role in the future sustainable society. The chemical and physical stability, on one hand, entails processing difficulties on the other hand. Wooden materials have been applied in many ways in our daily life, and are always present in our surroundings. Most of the wooden materials have been used without any chemical modification except for a few applications to make films and textiles. To explore more applications for wooden materials, we should understand the intrinsic characteristics of wooden components, especially cellulose and lignin, but a lack of good solvents made the molecular characterization of cellulose and lignin too complicated.

Solubility is essential for the molecular characterization, and is also required for shaping cellulose into films, fibers and other cellulosic bodies. However, as is widely known, cellulose is insoluble in water and common organic solvents. Despite of many attempts to understand its intrinsic property, there are still several aspects to be clarified with respect to an isolated cellulose molecule in solution in order to understand its nature better and this way advance its use in different applications.

In the past, chemical modification of cellulose has been performed in a semi-solid state, so that the outcome is a complex superposition of heterogeneous and homogenous derivatization, superimposed by different accessibilities, and thus reactivities, of amorphous and crystalline regions in cellulose. The chemical modification of cellulose will take place through the OH groups on the sugar backbone, so that the conformation of this cellulosic backbone with OH groups at C6, C3 and C3 determines the outcome of the chemical modification. In order to tailor a chemical modification, the conformational knowledge of an isolated chain may be crucial for its success.

Room-temperature ionic liquids (ILs) have been developed as solvents of cellulose (Swatloski et al. 2002). The mechanism of this dissolution process is not well understood, despite the increasing number of known ILs that are capable of dissolving cellulose (Heinze et al. 2005; Barthel and Heinze 2006; Fukaya et al. 2008). It has been also shown that the usually used imidazolium ionic liquids are not inert, but react with cellulose (Ebner et al. 2008), derivatizing the reducing ends and other carbonyl groups along the backbone (Rosenau et al. 2005). There have been many theoretical and experimental studies of cellulose dissolution in ILs, including NMR (Moulthrop et al. 2005; Youngs et al. 2011), viscosity (Gericke et al. 2009), electromagnetic wave scattering (Troshenkova et al. 2010; Chen et al. 2011) and molecular dynamics (Lynden-Bell et al. 2007; Liu et al. 2010; Rabideau et al. 2013; Zhao et al. 2013; Uto et al. 2018).

A cellulose chain in solution is generally described as a wormlike chain (semi-flexible chain) (Seger et al. 1996), but this model only affords a rough

approximation, like a molecule represented by a line. This wormlike chain model is not sufficient to produce understanding of the interaction between the cellulose molecule and the solvent, because the solvent effect is taken into account only indirectly through the semi-flexibility of a chain which yields a whole chain dimension in terms of the radius of gyration depending on the chain contour length (i.e. molecular weight). Here, we first focus on the conformation of cellulose in a local area in order to elucidate the state of solvation at the interface of the cellulosic chain with the bulk solvent by representing a local cellulosic chain with a simple rigid body. A mode of packing a cellulosic chain in a rigid body might indicate how the local conformation of a cellulosic chain could be and how the solvent molecules would surround a cellulosic chain.

Experimental

Cellulose samples

Chemicals were of the highest purity grade available and were used as received. *N*,*N*-Dimethylacetamide (DMAc) was obtained from LGC Promochem, Germany. Lithium chloride was purchased from BDH Prolabo by VWR International, Germany. Demineralized water was prepared by reverse osmosis. The ionic liquids (ILs), 1-ethyl-3-methylimidazolium acetate (EMIm-OAc) with purity 95%, 1-ethyl-3-methylimidazolium diethyl phosphate (EMIm-DEP) with purity 98%, and Avicel cellulose (PH101) was purchased from Sigma-Aldrich. The impurities of ionic liquids are mainly water and traces of imidazole (Im) and 1-methylimidazole (MIm) (Liebner et al. 2010).

Preparation of cellulose/IL solutions for GPC measurements

The solution was prepared by weighing cellulose directly in a sample bottle and adding ionic liquid to adjust the concentration of the solution to 5 wt%. Aging was performed in a drying oven at 353 K for specified times. Cellulose was recovered from the aged solution by reprecipitation with water, was separated by filtration, washed and subject to GPC characterization in order to evaluate a possible aging (chain degradation) effect.

GPC measurements

The system as described earlier (Henniges et al. 2011) was employed for the GPC measurement, where DMAc/LiCl (0.9%, m/V) was filtered through 0.02 µm filter and used as the eluent. The sample was injected automatically, chromatographed on four serial GPC columns, and monitored by Multi Angle Laser Light Scattering (MALLS) and refractive index (RI) detection. The molecular weight distribution and related polymer-relevant parameters were calculated by built-in software, by setting a refractive index increment to 0.136 mL/g for cellulose in DMAc/LiCl (0.9% m/V).

Preparation of cellulose/IL solutions for small-angle X-ray scattering (SAXS) measurements

The ILs were dried under vacuum for 2 h at 353 K before use. The sample solutions for SAXS were prepared by weighing cellulose directly in the sample bottle and adding solvent to adjust the concentration of the solutions. To ensure complete dissolution, the solution was heated for further 4 h at 353 K using a bath while the bath temperature was continuously monitored.

SAXS measurements

Synchrotron SAXS measurements were carried out at the beamline BL6A (Shimizu et al. 2013) at Photon Factory (PF), KEK (Tsukuba, Japan), and the beamline BL11 of SAGA-LS (Saga, Japan). An incident X-ray beam from synchrotron radiation was monochromatized to 0.150 nm (BL6A) or 0.155 nm (BL11), respectively. The scattered X-ray radiation was detected by the two-dimensional semiconductor detector (PILATUS3 1 M (BL6A), PILATUS 100 K (BL11)). The exact camera length was calibrated by using the diffraction peaks of silver behenate. The scattered X-ray radiation was detected every 1 min and accumulated to a total of 30 or 60 min. The solutions were injected into the Boron-Silicate capillary cells ($70 \times \phi$ $2.0 \times t$ 0.01 mm, WJM-Glas Müller GmbH, Germany) or the flat stainless-steel cells with quartz windows, mounted onto the cell

holder while keeping temperature at 298 K. The scattered intensities were corrected with respect to the variation of the incident X-ray flux by monitoring the beam with the ionizing chambers placed in front and back of the sample holder. The excess scattered intensities were evaluated by subtracting the scattered intensities of solvent from those of cellulose solutions. The scattering profile is observed by plotting the excess scattered intensities $I(q)$ against the scattering vectors q defined in terms of the scattering angle as:

$$q = \frac{4\pi}{\lambda}\sin\theta \quad (1)$$

with 2θ being the scattering angle specified by the vectors of the scattered and incident X-ray directions, and λ being the wave length.

Results and discussion

Aging effects

Cellulose is vulnerable to hydrolysis and/or oxidative chain cleavage at higher temperatures, an effect known as aging, and thus care should be taken to minimize such interference while preparing cellulose solutions. In order to evaluate the aging effect in the respective ILs, 5% cellulose IL solutions were prepared, and then the dissolved cellulose was recovered after a certain time of aging according to the procedure described above. The solvents used were EMIm-OAc and EMIm-DEP. The recovered cellulose samples were subjected to GPC-MALLS measurements to determine the molecular weight M_w, and the change of the cellulose molecular weight was observed as a function of aging times. Figure 1 shows the results of the cellulose Mw at different aging times at 353 K. At this temperature, the effect of aging became observable after 8 h as marked by a precipitous decrease of the cellulose molecular weight. That is, little degradation of cellulose would take place within 8 h of aging time in the IL at 353 K. Thus, subsequent SAXS measurements were always completed within 8 h after the preparation of the solutions in order to minimize a possible influence of cellulose degradation in IL on the scattering results.

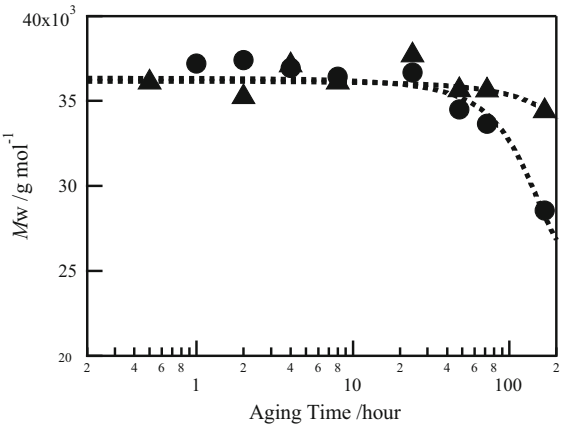

Fig. 1 Weight-average molecular masses of cellulose during aging in ionic liquids at 353 K. The circles and the triangles denote the solvents EMIm-OAc and EMIm-DEP, respectively. The determination of the molecular mass was carried with GPC using LiCl/DMAc as the eluent

Small-angle X-ray scattering (SAXS)

The influence of X-ray irradiation on cellulose integrity

Since the intensity of synchrotron radiation X-ray is powerful enough to damage organic materials, its energy could decompose and chemically affect of the IL and/or cellulose. Thus, the observed SAXS profile could be smeared by the fragmented and altered IL/cellulose. The time-resolved small-angle X-ray scattering (SAXS) data were observed every minute of X-ray irradiation. The SAXS profile from cellulose and IL started to change after 5 min of X-ray irradiation as seen Fig. 2. The incident X-ray intensities per minute are almost the same, because the measurements were done during top-up operation (operation with constant value of stored current) in PF. Since no irradiation influence on the scattering intensity was observed for IL solvents alone, the change in the SAXS intensities over time was evidently due to the chemical or structural change of cellulose by the impact of the strong synchrotron X-ray irradiation.

The scattered intensity at smaller q regions decreases consistently with time, indicating the degradation cellulose to a lower molecular weight. No change of the SAXS profile at higher q regions confirms the local cellulose conformation staying the same, and the peak in the intermediate q regions might suggest that the fragmented cellulose chains reacted

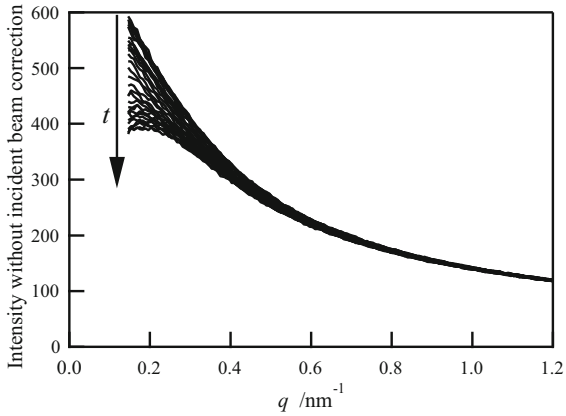

Fig. 2 Time-resolved SAXS raw intensities from the cellulose solution in the IL (EMIm-OAc). The time interval between the respective measurements is 1 min

with each other and formed a branched or coagulated structure (Henniges et al. 2012). Although we do not discuss the details of the decomposition mechanism of cellulose by X-ray irradiation in this paper, some experiments were performed to address this issue in a later report.

Observed SAXS profiles of cellulose IL solutions are consistent between two independent synchrotron facilities when the scattered intensities within the first 3 min of irradiation were compared, as shown in Fig. 3. The SAXS profiles were observed with different experimental set-ups at the PF and SAGA-LS sites. The measurements were thus confirmed to be reliable in terms of the data reproducibility, data acquisition, and sample stability during SAXS measurements.

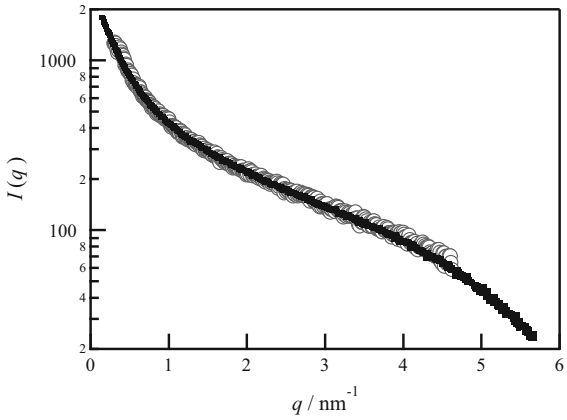

Fig. 3 SAXS profiles of cellulose in EMIm-OAc observed at two different synchrotron facilities. The data shown by open circles were observed at the SAGA-LS site, and the ones represented by small dots at the PF site

The effect of heat treatment on cellulose dissolution in the IL

A cellulose chain in solution is often modelled as a semi-flexible chain characterized by a persistence length. A persistent length specifies how stiff a chain is and is a length regarded as an extended straight (rigid) part of a chain. An alternative model for a semi-flexible chain is a broken-rod model where rigid cylinders are linked with flexible joints. When a molecule is rod-like, the scattering from such a molecule is approximately composed of two components representing the length of the rod and its cross-section, which is approximately described by the cross-sectional radius of gyration (Kajiwara and Wataoka 2016)

$$P_{cylinder}(q) \approx \frac{\pi}{2Hq} \cdot \exp\left(-\frac{q^2 R_c^2}{2}\right) \quad (2)$$

Here, $2H$ is the height of the cylinder, and R_c is the cross-sectional radius of gyration. This approximative relationship (the Guinier approximation for a cross-section) holds in the range where $qR_g \geq 1$ and $qR_c \leq 1$, and R_c is determined from the slope of $\ln\{qI(q)\}$ plotted against q^2 (referred to as the cross-sectional Guinier plots). This plot is shown in Fig. 4 for two cellulose/EMIm-OAc solutions prepared with heating at 353 K and without heating (dissolution at room temperature) in order to examine the heating

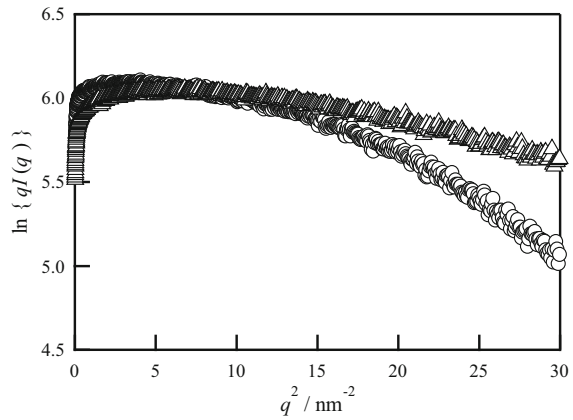

Fig. 4 Cross-sectional Guinier plots of the SAXS data observed from cellulose solutions in EMIm-OAc with (open circle) and without (open triangle) heating treatment

effect in the preparation of the sample solution. Here, the samples were prepared by dissolving the weighed celluloses at room temperature for 3 days or at 353 K in 6 h. A good linearity is to be expected from Eq. (2), and R_c could be evaluated approximately from the slope to be 0.23 nm in the q^2 range from 5 to 13 nm^{-2} in both solutions. The scattering profiles exhibit a large difference at larger q ranges beyond the valid region ($qR_c \geq 1$) for the cross-sectional Guinier approximation. The value of R_c estimated from the experimental results is nearly equal to R_c evaluated from the results of the molecular dynamics of cellulose oligomers (Chen et al. 2011). However, a detailed evaluation of Fig. 4 reveals a deviation from the linearity even in the range of q^2 from 5 to 13 nm^{-2} and a slight difference in the slopes of the solutions with and without heating. The consistency of the cross-sectional radius of gyration in the present SAXS results and the molecular dynamics for a single cellulose oligomer might indicate that cellulose molecules in the IL solutions used for the SAXS measurements are molecularly dispersed within the size scale observed by the present SAXS. The difference of the scattering profiles might be due to the state of dissolution of cellulose molecules in the IL with or without heating. It should be noted that a larger cross-sectional radius of gyration, 0.33 nm, is estimated for a single chain in a cellulose I crystal. Further discussion with regard to the conformation of cellulose molecules will be given below, employing more accurate models to better characterize the conformational change by heating.

The SAXS profiles at the larger q^2 regions reveal some differences. The difference is more enhanced in the Kratky plots shown in Fig. 5. When heated, a cellulose chain seems to have a thicker scattering unit than without heat treatment. The SAXS profile from a cellulose chain without heat treatment reveals a typical shape for a long, thin, rigid rod while the profile from the heat-treated solution exhibits a convex shape expected from a rather rigid body. As the cross-sectional radius of gyration does not change much by heating, these results indicate that the local conformation of cellulose in ionic liquid would not change depending on the conditions of dissolution. A remarkable difference in SAXS profiles at larger q region might be caused by a smaller structural unit such as a surface structure or solvation. Although it is reported that the cellulose dissolves but forms molecular

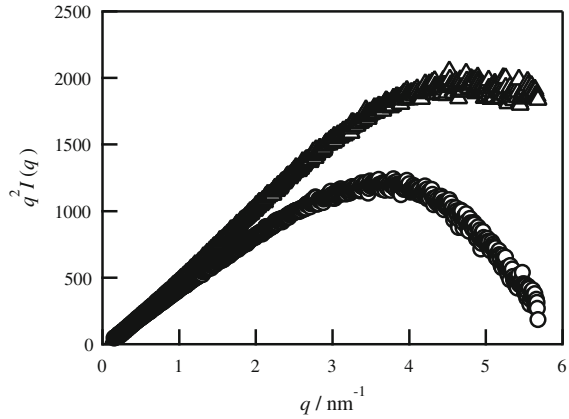

Fig. 5 Experimental SAXS profiles from cellulose with (open circle) and without (open triangle) heating during dissolution in EMIm-OAc. The concentration of the solute is 2 wt%

aggregates represented as a soft sphere (Troshenkova et al. 2010), the condition of dissolution in this paper were not clearly specified and no microscopic structural analysis was attempted. All structural evidence in the present experiments confirms that cellulose molecules are dissolved in the ILs without forming any aggregates when enough dissolution time was allowed with an appropriate heating treatment.

Model simulations for a cellulose chain in the IL solution

The following discussion is based on the results obtained from the heat-treated cellulose IL solutions, which exhibit the SAXS profiles shown in Figs. 4 and 5, denoted by open circles. The observed SAXS profiles are transformed into the electron distance correlation function, $P(r)$, in order to understand the shape of a cellulose molecule in IL solution, by the following expression.

$$P(r) = \frac{1}{2\pi^2}\int_0^\infty I(q)\cdot qr\cdot \sin(qr)dq \qquad (3)$$

The distance correlation function $P(r)$ transformed from the observed SAXS profile is characterized by a peak at a shorter distance and a longer tail at longer distances, revealing the characteristics of a cylinder (see the solid line in Fig. 6): The peak corresponds to the cross-section and a long tail to the length of the cylinder in a rough description of the distance correlation function. The correlation function could be approximately fit to a homogeneous cylinder of a

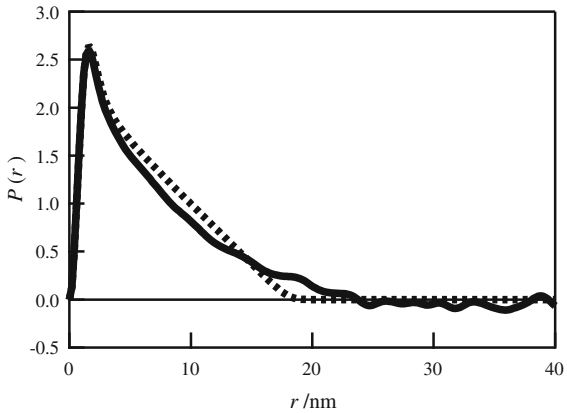

Fig. 6 Electron distance distribution function estimated from the simple cylinder model of a radius r = 0.31 nm and a length $2H$ = 9.0 nm (dashed line) and the observed SAXS profile from cellulose in EMIm-OAc solution (solid line). The concentration of solute is 2 wt%

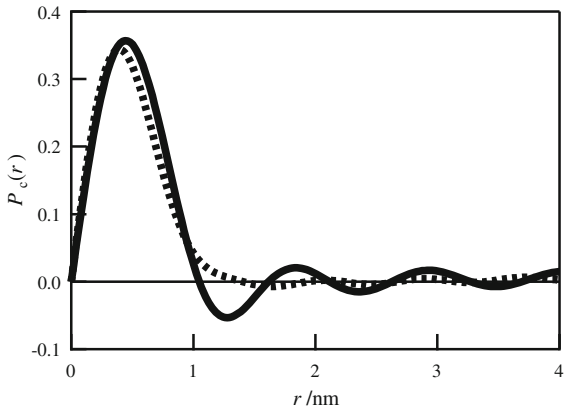

Fig. 7 Cross-sectional electron distance distribution function calculated from a cylinder model (dashed line, cf. also Fig. 6) and converted from the observed SAXS profiles of a 2 wt% cellulose solution in EMIm-OAc (solid line)

radius r = 0.31 nm and a length $2H$ = 9.0 nm (see the dashed line in Fig. 6). The deviation of the real data from an ideal rigid cylinder model is due to the semi-flexibility of a real cellulose chain and/or the effect of solvation.

In order to understand the interaction of a cellulosic chain with the surrounding solvent, the electron distance distribution with regard to the radial direction around the cellulose cross-section should be evaluated. The electron distance distribution in the radial direction can be calculated with the Henkel transform from the cross-sectional parts of the scattering profile according to Eq. (4) (Glatter 1983).

$$P_c(r) = \frac{1}{2\pi}\int_0^\infty I_c(q)\cdot qr\cdot J_0(qr)dq \tag{4}$$

from the experimental data as shown in Fig. 7, the most characteristic difference is that $P_c(r)$ transformed from observed SAXS data takes a negative value while that from a rigid cylinder falls asymptotically to zero as expected. The negative value in the electric distance distribution function indicates the lower electron density than that of solvent, and the layer of lower electron density surrounds the core consisted of a cellulosic chain which is characterized by a higher electron density. A molecular model to satisfy this phenomenon of an apparent negative electron density could be represented by a double layer of different electron densities, assuming a coaxial cylindrical structure, i.e. being composed of a sheath and a core.

The particle scattering function from a coaxial double cylinder model is given as (Livsey 1987)

$$P(q) = \int_0^{\frac{\pi}{2}} \left| \frac{\Delta\rho_{in} r_{in}^2 2\pi h\cdot G(q,\beta;r_{in}) + \Delta\rho_{out} r_{out}^2 2\pi h\cdot G(q,\beta;r_{out}) + \Delta\rho_{out} r_{in}^2 2\pi h\cdot G(q,\beta;r_{in})}{(\Delta\rho_{in}-\Delta\rho_{out}) r_{in}^2 2\pi h + \Delta\rho_{out} r_{out}^2 2\pi h} \right|^2 \times \sin\beta d\beta \tag{5}$$

where $J_0(qr)$ is a zero-order Bessel function, and $I_c(q)$ is the scattering intensity of cross-section. When the electron distance correlation function of cross-section, $P_c(r)$, calculated from a homogeneous cylinder model is compared with the profile transformed

where $\Delta\rho_{\mathrm{in}}$ and $\Delta\rho_{\mathrm{out}}$ are the difference of electron density between solvent and inner-cylinder as well as outer-cylinder specified by the radius r_{in} and r_{out}, respectively. The function G(q,β; x) is defined as

$$G(q,\beta;x) = \frac{\sin(2\pi Hq\cdot\cos\beta)\cdot 2J_1(qx\sin\beta)}{(2\pi Hq\cdot\cos\beta)(qx\sin\beta)} \qquad (6)$$

where H is the cylinder half-length and $J_1(S)$ is a first-order Bessel function of an argument S. The observed scattering profile was simulated according to Eq. (5) by fitting the observed profiles with three parameters; the inner radius r_{in} and the outer radius r_{out} of the cylinder, and by setting $\Delta\rho_{in} - \Delta\rho_{out} = 1$. The cylinder length $2H$ does not reflect a whole cellulose chain in fitting since the range observed by SAXS covers only a part of a long cellulose chain, and this range is represented by a cylinder. The model cylinder might be related to a cellulosic chain of a persistent length specified by a semi-flexible chain model.

Figure 8 shows the fitting results and the parameters used in Eq. (5) which are summarized in Table 1. The inner radius of the model cylinder for a cellulosic chain after heat-treatment is around 0.50 nm (0.35 nm in terms of the cross-sectional radius of gyration), which is consistent with the cross-sectional radius estimated for a single cellulose chain in the cellulose crystal I., but larger than that evaluated from the molecular dynamics for a single cellulose oligomer in water or EMIm-OAc or that from a simple cross-sectional Guinier plot (see Fig. 4). However, the inner radius of the model cylinder for a cellulosic chain before heat-treatment is as small as 0.36 nm (0.25 nm in terms of the cross-sectional radius of gyration), which is equivalent to the cross-sectional diameter estimated from the molecular dynamics in EMIm-OAc.

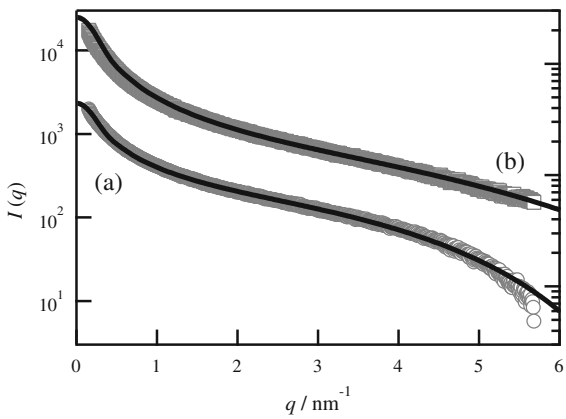

Fig. 8 SAXS profiles calculated with a coaxial double cylinder model (solid line). The experimental SAXS profiles originate from cellulose dissolved in EMIm-OAc and then (a) heat-treated (circles) or (b) without heat-treatment (squares). The upper profile (squares) was shifted for better comparison. The concentration of solute is 2 wt%

The core of a coaxial double cylinder is considered as consisting of a cellulosic chain, and the conformation of the cellulosic chain determines the cross-sectional radius. When cellulose is dissolved in EMIm-OAc, the cellulosic chain assumes the conformation as simulated by molecular dynamics. Heating promotes the rearrangement of a cellulosic chain by breaking intramolecular interactions and the conformation would change accordingly, with a new minimal potential condition. The cellulosic chain is solvated with EMIm-OAc molecules which constitute an outer layer (sheath) in a coaxial double cylinder model. The lower electron density in the outer layer indicates that EmimAc molecules are not so tightly packed in the solvation layer, probably due to restricted numbers of specific sites of a cellulosic chain which interact with ionic liquids. Ionic liquids prevent the intermolecular and intra-molecular hydrogen bonding of cellulosic chains. In consequence, the packing density in this layer is lower than in bulk, resulting in a lower electron density.

When the cellulose solution was not heat-treated in prior to the SAXS measurements, the simulated coaxial double cylinder model yields a smaller cross-sectional radius and a thinner sheath layer. The electron density difference of the sheath layer is almost negligible, that is, it is almost the same as bulk solvent. The results are summarized in Table 1 and Fig. 8. The cross-sectional radius of the core is equivalent to the radius evaluated from the simulated cellulose oligomer in EMIm-OAc. Here, the cellulosic chain is free from any interaction and its conformation is determined by minimizing the intramolecular potential of an isolated (oligomeric) chain. The smaller cross-sectional radius reflects the extended chain structure of cellulose, which could provide more sites available for solvent interactions. More EMIm-OAc molecules are present in the surroundings of a cellulosic chain in the non-heated solutions than in the heat-treated solutions, resulting in the higher electron density of the former (almost the same as bulk solvent) in comparison to the latter solution. Heating promotes the molecular motion of a cellulosic chain, and its conformation settles in another energy minimum, probably more stable, through the interaction with solvent molecules.

Table 1 Optimized parameters in a coaxial double cylinder model by fitting to the experimental SAXS profiles

	r_{in} (nm)	r_{out} (nm)	$r_{out} - r_{in}$ (nm)	ρ_{in}	ρ_{out}	H (nm)
In EMIm-OAc with heating	0.54	0.95	0.41	0.86	− 0.24	5.0
In EMIm-OAc without heating	0.36	0.74	0.38	0.93	− 0.07	4.0
In EMIm-DEP with heating	0.46	1.12	0.66	0.92	− 0.08	3.2

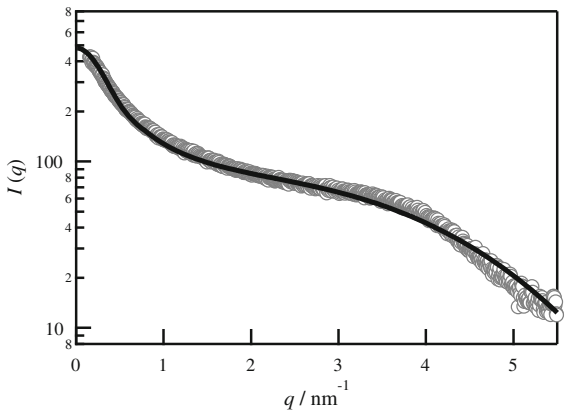

Fig. 9 SAXS profiles calculated by a coaxial double cylinder model (solid line) and experimental (circles) SAXS from cellulose dissolved in EMIm-DEP. The concentration of solute is 2 wt%

Another ionic liquid (results not shown) yielded similar results, also modelled by a coaxial double layer cylinder. Figure 9 shows the scattering profile from cellulose in EMIm-DEP solution. The fitting curve was again calculated from the corresponding coaxial double cylinder model. A similar model was applied to the SAXS profile observed form the cellulose/EMIm-DEP solution, and the parameters to specify this model are not fundamentally different from those evaluated for the system cellulose/EMIm-OAc. Since the molecular size of EMIm-DEP is larger than that of EMIm-OAc, the sheath thickness was consequently found to be larger than that of cellulose/EMIm-OAc solution. Considering that the electron density difference is almost negligible, the electron density of the solvent surrounding a cellulosic chain is similar to that of bulk solvent. The cross-sectional radius in this system takes a value between heat-treated cellulose/EMIm-OAc solution and not heat-treated one. The cellulosic chain is moderately extended and provides sufficient sites for solvent molecules to be accommodated. The conformation of cellulosic chain is thus less extended than that in not heat-treated EMIm-OAc solution. The sheath layer is thicker because of the larger size of the EMIm-DEP molecule. The fitting of the coaxial double cylinder model to the observed SAXS profile is reasonable, and the cellulosic chain is relatively extended as approximately modelled by a coaxial double cylinder. The results are summarized in Fig. 9 and Table 1.

Conclusions

Cellulose dissolved in EMIm-OAc suffers from degradation at elevated temperatures for prolonged times. All the SAXS measurements were completed within 8 h from the preparation of respective solutions at 353 K; a period of time for which cellulose degradation was shown to be insignificant. Cellulose was found to be dissolved as individual chains in EMIm-OAc, but the conformation changed by heat treatment. A coaxial double cylinder model was adapted to represent a local structure of a dissolved cellulosic chain, which exhibited an unusual behavior of the scattering profiles expected from a conventional rod-like molecule. In the present work, the SAXS profiles from cellulose/EMIm-OAc solutions are well simulated by a coaxial double cylinder model where the sheath (an outer shell) and the core (an inner part) are constituted of EMIm-OAc or EMIm-DEP solvent molecules and the solute cellulose, respectively. The electron density of the sheath varies according to the packing state of solvent molecules, which is determined by the conformation of cellulose in the core providing the sites suitable for the interaction with the solvents. Although it is rather simple, the coaxial double cylinder model represents the local structure of a cellulosic chain in the solvents quite well, and indicates the mode of solvation. The thickness of the sheath in the coaxial double cylinder corresponds to the size of a solvent molecule, and the cylinder length corresponds to the range of a rigid rod approximation

as specified by a persistent length in the conventional semi-flexible chain model.

Acknowledgments This work was performed under the approval of the Photon Factory Program Advisory Committee (Proposal Nos. 2014G604 and 2015G147) and the approval of the SAGA-LS (Proposal No. 1403013R). This work was financial supported by the Center for Fiber Textile Science in Kyoto Institute of Technology, and the Division of Chemistry of Renewable Resources, BOKU University Vienna. We gratefully acknowledge the work of past and present members of our laboratories.

References

Barthel S, Heinze T (2006) Acylation and carbanilation of cellulose in ionic liquids. Green Chem 8:301–306

Chen Y, Zhang Y, Ke F, Zhou J, Wang H, Liang D (2011) Solubility of neutral and charged polymers in ionic liquids studied by laser light scattering. Polymer 52:481–488

Ebner G, Schiehser S, Potthast A, Rosenau T (2008) Side reaction of cellulose with common 1-alkyl-3-methylimidazolium-based ionic liquids. Tetrahedron Lett 49:7322–7732

Fukaya Y, Hayashi K, Wada M, Ohno H (2008) Cellulose dissolution with polar ionic liquids under mild conditions: required factors for anions. Green Chem 10:44–46

Gericke M, Schlufter K, Liebert T, Heinze T, Budtova T (2009) Rheological properties of cellulose/ionic liquid solutions: from dilute to concentrated states. Biomacromolecules 10:1188–1194

Glatter O (1983) Data treatment. In: Gratter O, Kratky O (eds) Small angle X-ray scattering. Academic Press, New York, pp 119–165

Heinze T, Schwikal K, Barthel S (2005) Ionic liquids as reaction medium in cellulose functionalization. Macromol Biosci 5:520–525

Henniges U, Kostic M, Borgards A, Rosenau T, Potthast A (2011) Dissolution behavior of different celluloses. Biomacromolecules 12:871–879

Henniges U, Okubayashi S, Rosenau T, Potthast A (2012) Irradiation of cellulosic pulps: understanding its impact on cellulose oxidation. Biomacromolecules 13(12):4171–4178

Kajiwara K, Wataoka I (2016) The method of small-angle X-ray scattering and its application to the structural analysis of oligo- and polysaccharides in solution. In: Matricardi P, Alhaique F, Coviello T (eds) Polysaccharide hydrogels: characterization and biomedical applications. Pan Stanford Publishing, Singapore, pp 265–323

Liebner F, Ebner G, Becker E, Potthast A, Rosenau T (2010) Thermal aging of 1-alkyl-3-methylimidazolium ionic liquids and its effect on dissolved cellulose. Holzforschung 64:161–166

Liu H, Sale KL, Holmes BM, Simmons BA, Singh S (2010) Understanding the interactions of cellulose with ionic liquids: a molecular dynamics study. J Phys Chem B 114:4293–4301

Livsey I (1987) Neutron scattering from concentric cylinders. J Chem Soc Faraday Trans 2 83:1445–1452

Lynden-Bell RM, Del Popolo MG, Youngs TG, Kohanoff J, Hanke CG, Harper JB, Pinilla CC (2007) Simulations of ionic liquids, solutions, and surfaces. Acc Chem Res 40:1138–1145

Moulthrop JS, Swatloski RP, Moyna G, Rogers RD (2005) High-resolution 13C NMR studies of cellulose and cellulose oligomers in ionic liquid solutions. Chem Commun (Camb) 12:1557–1559

Rabideau BD, Agarwal A, Ismail AE (2013) Observed mechanism for the breakup of small bundles of cellulose Ialpha and Ibeta in ionic liquids from molecular dynamics simulations. J Phys Chem B 117:3469–3479

Rosenau T, Potthast A, Kosma P, Saariaho AM, Vuorinen T, Sixta H (2005) On the nature of carbonyl groups in cellulosic pulps. Cellulose 12:43–50

Seger B, Aberle T, Burchard W (1996) Solution behaviour of cellulose and amylose in iron-sodiumtartrate (FeTNa). Carbohydr Polym 31:105–112

Shimizu N, Mori T, Igarashi N, Ohta H, Nagatani Y, Kosuge T, Ito K (2013) Refurbishing of small-angle X-ray scattering beamline, BL-6A at the photon factory. J Phys Conf Ser 425:202008

Swatloski RP, Spear SK, Holbrey JD, Rogers RD (2002) Dissolution of cellulose with ionic liquids. J Am Chem Soc 124:4974–4975

Troshenkova SV, Sashina ES, Novoselov NP, Arndt KF (2010) Light scattering in diluted solutions of cellulose and hydroxypropylcellulose in 1-ethyl-3-methylimidazolium acetate. Russ J Gen Chem 80:501–506

Uto T, Yamamoto K, Kadokawa J (2018) Cellulose crystal dissolution in imidazolium-based ionic liquids: a theoretical study. J Phys Chem B 122:258–266

Youngs TGA, Holbrey JD, Mullan CL, Norman SE, Lagunas MC, D'Agostino C, Mantle MD, Gladden LF, Bowron DT, Hardacre C (2011) Neutron diffraction, NMR and molecular dynamics study of glucose dissolved in the ionic liquid 1-ethyl-3-methylimidazolium acetate. Chem Sci 2:1594–1605

Zhao Y, Liu X, Wang J, Zhang S (2013) Effects of anionic structure on the dissolution of cellulose in ionic liquids revealed by molecular simulation. Carbohydr Polym 94:723–730